ELSEVIER

Coordination Chemistry Reviews
176 (1998) 67–86

COORDINATION CHEMISTRY REVIEWS

Aminotroponiminato complexes of silicon, germanium, tin and lead

H.V. Rasika Dias*, Ziyun Wang, Wiechang Jin

Department of Chemistry and Biochemistry, Box 19065, The University of Texas at Arlington, Arlington, TX 76019-0065, USA

Received 2 October 1997; accepted 6 January 1998

Contents

Abstract

Aminotroponiminates are very useful ligands in group 14 chemistry. They readily form complexes with both low and high valent group 14 metal ions. Synthesis, structural features and some chemistry of aminotroponiminato silicon, germanium, tin and lead derivatives are reviewed.

Keywords: Aminotroponiminates; Ligands

1. Introduction

Aminotroponimines (e.g. **1**) are an interesting group of bidentate, nitrogen donor ligands. Although aminotroponimines are structurally similar to tropolone (**2**),

* Corresponding author. Tel.: +1 817 2723813; fax: +1 817 2723808; e-mail: dias@uta.edu

0010-8545/98/$ - see front matter
PII S0010-8545(98)00112-X

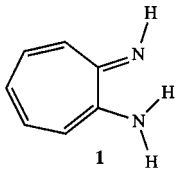

1
aminotroponimine

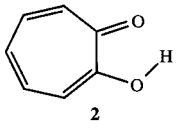

2
tropolone

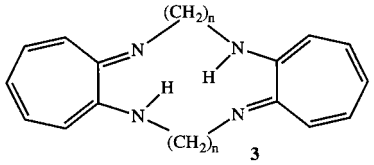

3
tropocoronands

various physical and chemical data indicate significant differences between the two types [1,2]. For example, aminotroponimines contain a highly delocalized 10-electron π-system delocalized over seven carbons and the two nitrogen atoms. In contrast, properties of tropolone are best understood in terms of a π-system involving only six electrons. Furthermore, unlike tropolone, the steric and electronic properties of aminotroponimines may be easily modulated by changing the substituent on nitrogen (or on the ring carbon atom). In fact, a variety of *N,N′*-disubstituted aminotroponimines including the closely related tropocoronands (**3**) are known [1–12].

Aminotroponiminate ligands $[(R)_2ATI]^-$ (**4**), which are formally derived from aminotroponimines $[(R)_2ATI]H$ by deprotonation, can also be compared to amidinates (**5**) [13] and β-diketinimates (**6**) [4,14]. All three types are nitrogen based, bidentate, monoanionic and formally four-electron donor ligand systems. However, upon coordination to metal ions, aminotroponiminates form a five-membered chelate ring whereas amidinates and β-diketinimates form four and six-membered metallacycles, respectively. Furthermore, unlike the aminotroponiminate which features a delocalized 10π electron ligand backbone, amidinates and β-diketinimates have delocalized 4π and 6π electron ligand backbones. Among the three types, amidinates have been the most widely used in coordination chemistry

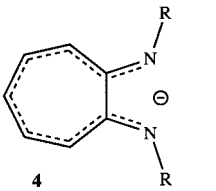

4
Aminotroponiminate, $[(R)_2ATI]^-$
10π electron system

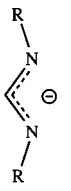

5
Amidinate
4π electron system

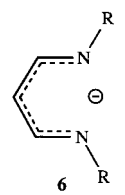

6
β-Diketinimates
6π electron system

whereas aminotroponiminates and β-diketinimates have received relatively less attention [4,13,14].

Studies involving aminotroponiminate ligand (including those of the related tropocoronand) have mostly been limited to the first row, middle and late transition metal ions, such as manganese, iron, cobalt, nickel, copper and zinc [2,4,5,10,15–25]. Aminotroponiminates have also been used as ancillary ligands (particularly as an alternative to cyclopentadienyl ligand) in early transition metal chemistry [26–28]. This article will review the use of aminotroponimines in group 14 chemistry which represents an area of increasing activity recently [12,29,30]. The main focus will be on the synthesis, structures and chemistry of compounds involving silicon, germanium, tin and lead, and the related starting materials.

2. The starting materials

The first report of an aminotroponimine appeared in 1953, which concerns the synthesis of amino derivative **7** using tropolone [31]. The synthesis of *N,N′*-dibenzoyl analog **8** starting from diazaazulene has also been reported [32]. The parent compound 1-amino-7-imino-1,3,5-cycloheptatriene (**1**) was later prepared by reacting tetrafluorocycloheptadienes (obtained using cyclopentadiene and tetrafluoroethylene) [33] with ammonia (Eq. 1; where R = H) [3]. Similarly, a large number of *N,N′*-disubstituted aminotroponimines ([$(R)_2$ATI]H; where R = methyl, *i*-butyl, benzyl, phenyl, *p*-tolyl, *p*-methoxyphenyl, *p*-chlorophenyl, *p*-dimethylaminophenyl, *p*-phenylazophenyl, *p*-nitrophenyl and several others) have also been synthesized using primary amines instead of ammonia in the above reaction scheme [2,3]. The product yields range from 30 to 80%. Relatively more convenient and high-yield synthetic routes to *N,N′*-disubstituted aminotroponimines (particularly *N*-alkyl derivatives) are now available [6,7,11,12,16,34–37]. These methods mainly use easily

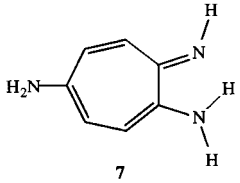

7

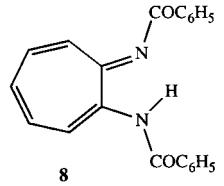

8

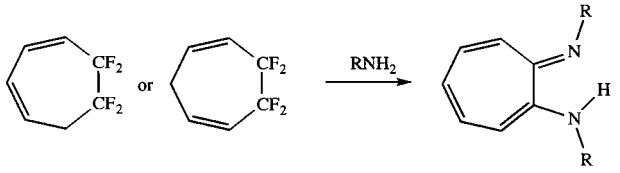

(1)

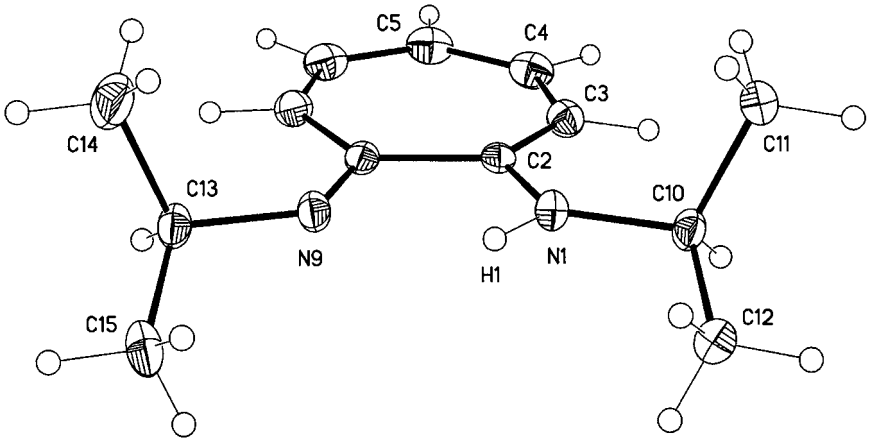

Fig. 1. Molecular structure of $[(i\text{-Pr})_2\text{ATI}]H$. Reprinted with permission from Dias et al. [11] © 1995 American Chemical Society. Selected bond lengths (Å) and angles (°): N1–C2, 1.342(3); N9–C8, 1.314(3); C2–N1–C10, 126.6(2); C8–N9–C13, 122.1(3); N1–C2–C8, 111.7(2); N9–C8–C2, 122.8(3).

accessible tropolone or tropolone derivatives as starting material rather than tetrafluorocycloheptadienes.

Aminotroponimines are brightly colored, crystalline solids. Colors typically range from yellow to brick-red depending on the substituent on nitrogen. NMR spectroscopic data of $[(Me)_2\text{ATI}]H$ are indicative of a C_2-symmetric structure in solution even at −80°C [2,38]. Solid state and solution IR spectroscopic studies indicate intramolecular H-bonding in $[(Me)_2\text{ATI}]H$ [1,2]. Several aminotroponimines, $[(R)_2\text{ATI}]H$ where R = Me, α-methylbenzyl and *i*-propyl, have also been charac-

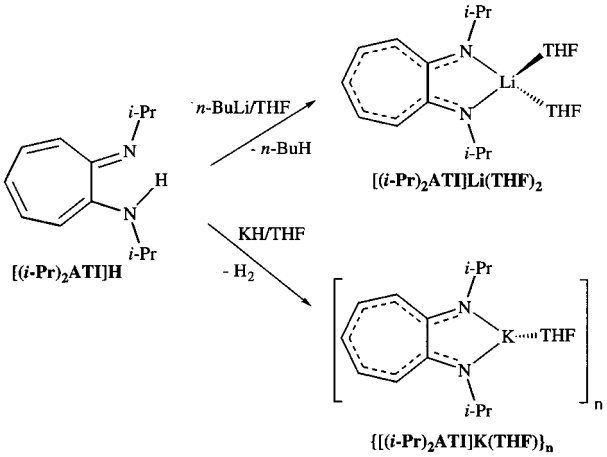

(2)

terized by X-ray crystallography [11,38,39]. $[(Me)_2ATI]H$ shows a C_2-symmetric structure with equivalent C_{ring}–N distances [38]. However, in the latter two structures, C_{ring}–N distances are not equal (for R = α-methylbenzyl; 1.355(4), 1.305(4) Å [39] and for R = *i*-propyl; 1.342(3), 1.314(3) Å [11]) indicating the presence of an amino nitrogen (C-N(R)H) with a strong N–H interaction and an imino nitrogen center (C = NR). The ORTEP diagram of $[(i\text{-}Pr)_2ATI]H$ is illustrated in Fig. 1. The seven-membered ring, two nitrogens, C10 and C13 occupy a single plane. The isopropyl groups orient in a manner that minimizes the steric interaction with the two hydrogens on C3 and C7.

The alkali metal salts can be obtained conveniently by treating aminotroponimines with appropriate bases [26,40–43]. For example, $[(i\text{-}Pr)_2ATI]Li$ and $[(i\text{-}Pr_2ATI]K$ were obtained by treating $[(i\text{-}Pr)_2ATI]H$ with Bu^nLi or KH (Eq. 2). They are very air sensitive solids. The X-ray crystal structures of $[(i\text{-}Pr_2ATI]Li(THF)_2$ and $\{[(i\text{-}Pr)_2ATI]K(THF)\}_n$ are known [26,42]. The lithium derivative adopts a monomeric structure (Fig. 2) whereas the potassium salt displays an interesting chain structure which features a π-bonded aminotroponimine ring (Fig. 3). The $N–C_{ring}$ bond distances of $[(i\text{-}Pr)_2ATI]Li(THF)_2$ and $\{[(i\text{-}Pr)_2ATI]K(THF)\}_n$ are much closer to the imine $N = C_{ring}$ distance in the free ligand. These alkali metal derivatives serve as versatile reagents for the introduc-

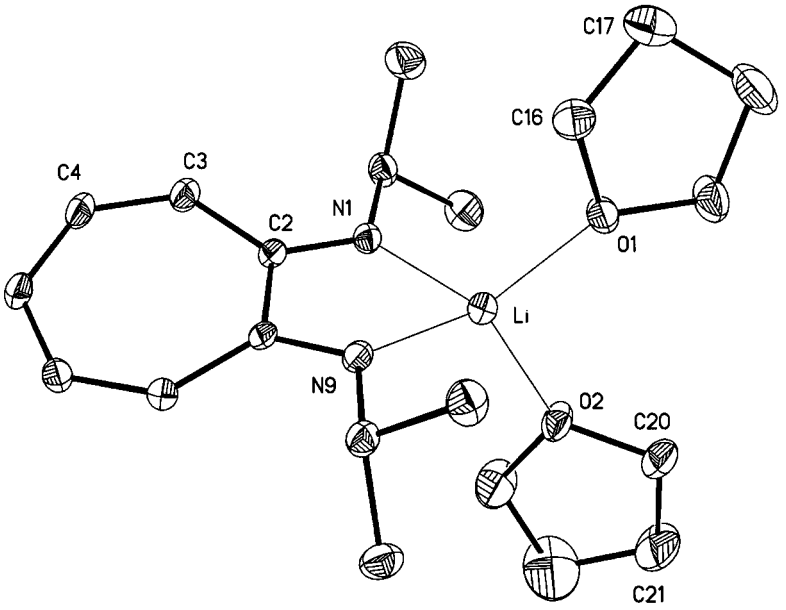

Fig. 2. Molecular structure of $[(i\text{-}Pr)_2ATI]Li(THF)_2$. Reprinted with permission from Dias et al. [26] © 1996 American Chemical Society. Selected bond lengths (Å) and angles (°): Li–N1, 1.995(6); Li–N9, 1.990(6); Li–O, 1.971(6); Li–O2, 1.960(6); N1–C2, 1.313(4); N9–C8, 1.319(4); N1–Li–N9, 81.5(2); O1–Li–O2, 118.3(3); C2–N1–Li, 114.0(3); C8–N9–Li, 113.4(3); N1–C2–C8, 114.4(3); N9–C8–C2, 113.7(3).

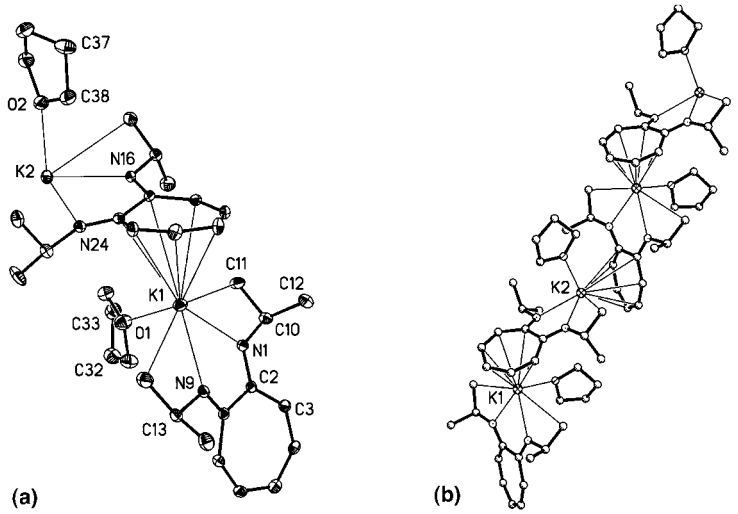

Fig. 3. Molecular structure of $\{[(i\text{-Pr}_2\text{ATI}]\text{K(THF)}\}_n$. **A**. ORTEP diagram showing the atom numbering scheme. **B**. A view showing the polymeric chain structure. Selected bond lengths (Å) and angles (°): K1–O1, 2.690(4); K1–N1, 2.717(4); K1–N9, 2.741(4); N1–C2, 1.312(6); N9–C8, 1.321(6); K2–O2, 2.657(4); K2–N16, 2.712(4); K2–N24, 2.730(4); N16–C17, 1.304(6); N24–C23, 1.307(6); N1–K1–N9, 58.72(12); N16–K2–N24, 58.93(12).

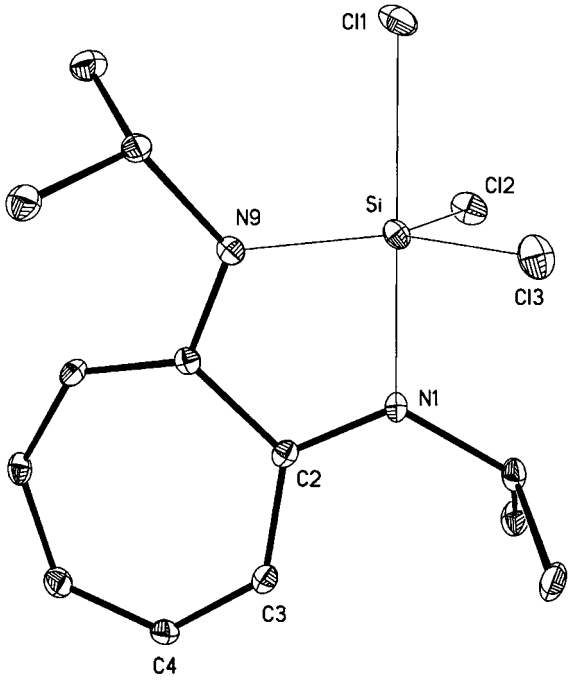

Fig. 4. Molecular structure of $[(i\text{-Pr})_2\text{ATI}]\text{SiCl}_3$. Selected bond lengths (Å) and angles (°): Si–N1, 1.870(2); Si–N9, 1.773(3); Si–Cl1, 2.1999(11); Si–Cl2, 2.1069(11); Si–Cl3, 2.0905(12); N1–C2, 1.331(4); N9–C8, 1.381(4); N1–Si–N9, 85.46(11); N1–Si–Cl1, 178.07(9); N9–Si–Cl1, 90.19(5); N9–Si–Cl2, 120.34(9); N9–Si–Cl3, 123.51(9); Cl2–Si–Cl3, 115.97(5).

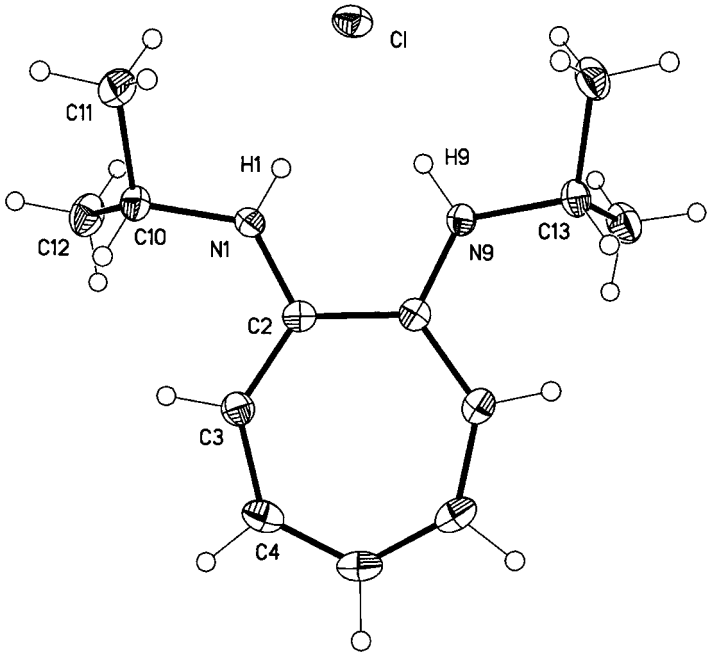

Fig. 5. Molecular structure of $\{[(i\text{-Pr})_2\text{ATI}]H_2\}^+Cl^-$. Selected bond lengths (Å) and angles (°): N1–C2, 1.343(2); N9–C8, 1.342(2); C2–N1–C10, 126.4(2); C8–N9–C13, 125.9(2); N1–C2–C8, 117.0(2); N9–C8–C2, 117.2(2).

tion of aminotroponiminato moiety to various metal ions. Lithium salts thus far have been the reagents of choice for group 14 derivatives.

3. Aminotroponiminato complexes of heavier group 14 elements

In 1964 and 1965, Muetterties reported the synthesis of several compounds of the type $\{[(R)_2\text{ATI}]_3M\}^+X^-$ (where R = mainly Me; M = Si, Ge, or Sn; X = halide, PF_6, etc.) by treating the corresponding tetrahalides with $[(R)_2\text{ATI}]H$ or its lithium salt [40,44]. These crystalline compounds were characterized by elemental analysis and believed to contain octahedral metal centers. Interestingly, regardless of the metal/ligand ratio, the tris-ligand complex was the only product isolated. The tetrakis analogs could not be obtained due to the unfavorable steric interactions between substituents on nitrogen atoms. $[(R)_2\text{ATI}]_3M^+X^-$ compounds are stable in aqueous alkaline solutions. However, they rapidly degrade in acidic media leading to the formation of acid salts of free ligands, e.g. $\{[(R)_2\text{ATI}]H_2\}^+Cl^-$ [40].

With more bulky ligands, monosubstituted derivatives can be obtained. For example, it was possible to synthesize $[(i\text{-Pr})_2\text{ATI}]SiCl_3$ by treating $[(i\text{-Pr})_2\text{ATI}]Li$ with $SiCl_4$ [42]. It was characterized by NMR spectroscopy and X-ray crystallogra-

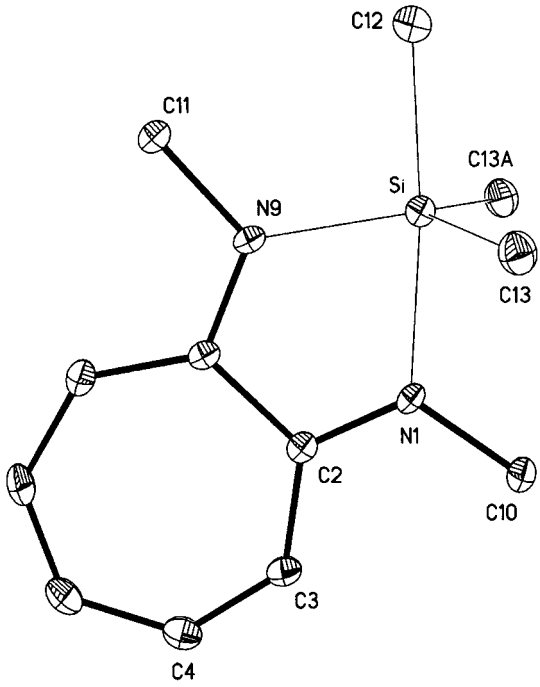

Fig. 6. Molecular structure of $[(Me)_2ATI]SiMe_3$. Selected bond lengths (Å) and angles (°): Si–N1, 2.037(4); Si–N9, 1.848(4); Si–C13, 1.890(4); Si–C13A, 1.890(4); Si–C12, 1.927(6); N1–C2, 1.308(6); N9–C8, 1.359(6); N1–Si–N9, 77.8(2); N9–Si–C12, 96.8(2); N1–Si–C12, 174.6(2); N9–Si–C13, 118.38(14); C13–Si–C13A, 120.2(3).

phy (Fig. 4). The silicon atom adopts a trigonal bipyramidal geometry with nitrogen atoms of the aminotroponiminate ligand occupying one axial [with Si–N distance of 1.870(2) Å] and one equatorial site [Si–N = 1.773(3) Å]. $[(i\text{-}Pr)_2ATI]SiCl_3$ decomposes upon exposure to moisture and $\{[(i\text{-}Pr)_2ATI]H_2\}^+Cl^-$ was observed among the decomposition products [42]. In contrast to the free ligand $[(i\text{-}Pr)_2ATI]H$, this HCl salt displays a fairly symmetric C_7N_2 moiety in the solid state (Fig. 5) with two equal C_{ring}–N distances of 1.343(2) and 1.342(2) Å. These distances are similar to the amine C_{ring}–N bond length of the free ligand. The chloride ion shows hydrogen bonding to protons on the two nitrogen atoms.

The tin(IV) compound $[(Et)_2ATI]SnPh_3$ has been prepared by the reaction of $[(Et)_2ATI]Li$ with Ph_3SnCl [41]. The corresponding germanium and silicon analogs are significantly more reactive, and have not been isolated in pure form. These compounds decompose rapidly in the presence of moisture. The reaction between Me_3SnCl or Me_3SiCl with $[(Me)_2ATI]Li$ gives corresponding Sn(IV) or Si(IV) derivatives (Eq. 3) [45]. These adducts have been characterized by NMR spectroscopy and X-ray crystallography. $[(Me)_2ATI]SiMe_3$ (Fig. 6) and $[(Me)_2ATI]SnMe_3$ (Fig. 7) have very similar solid state structures which feature five-coordinate,

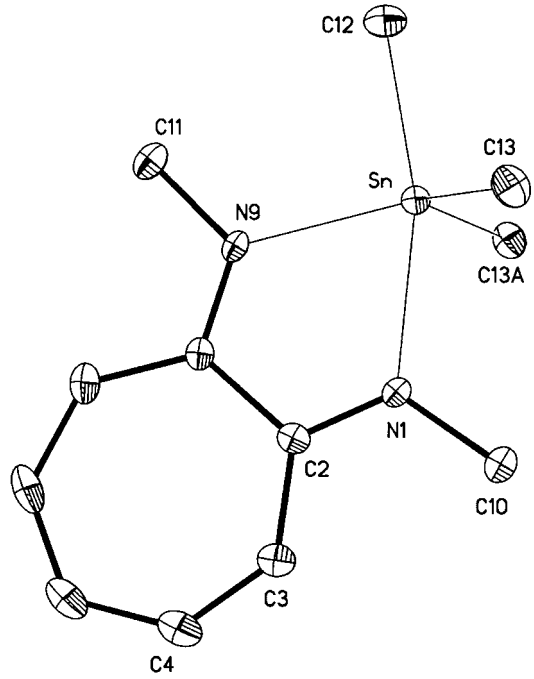

Fig. 7. Molecular structure of $[(Me)_2ATI]SnMe_3$. Selected bond lengths (Å) and angles (°): Sn–N1, 2.281(4); Sn–N9, 2.173(4); Sn–C13, 2.145(4); Sn–C13A, 2.145(4); Sn–C12, 2.179(6); N1–C2, 1.302(7); N9–C8, 1.342(7); N1–Sn–N9, 70.2(2); N9–Sn–C12, 94.8(2); N1–Sn–C12, 165.1(2); N9–Sn–C13, 118.06(11); C13–Sn–C13A, 117.9(2).

trigonal bipyramidal metal sites [45]. The tin analog shows relatively longer metal–N and metal–C distances (as expected based on the larger atomic radius of Sn). The N1–Sn–C12 bond angle of $[(Me)_2ATI]SnMe_3$ is approx. 10° smaller than the related N1–Si–C12 angle of $[(Me)_2ATI]SiMe_3$. These two compounds show fluxional behavior in solution at room temperature. For example, only a single N–Me (or M–Me) resonance was found in the ^1H NMR spectrum of $[(Me)_2ATI]SiMe_3$ or $[(Me)_2ATI]SnMe_3$. The ^1H NMR spectrum of

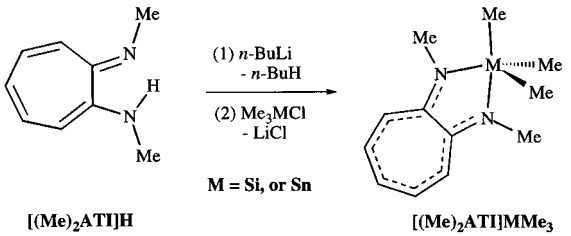

(3)

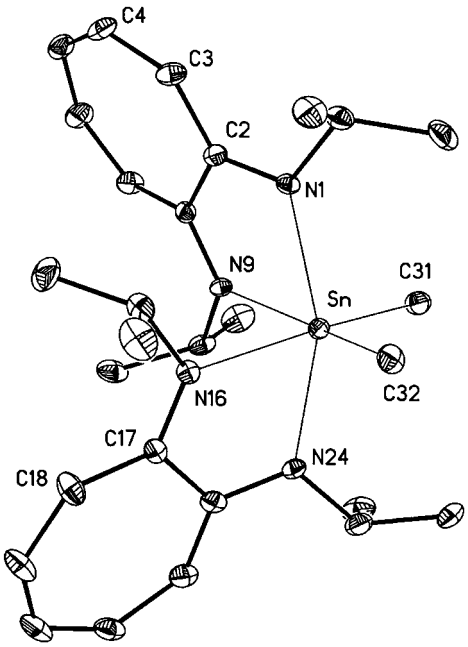

Fig. 8. Molecular structure of $\{[(i\text{-Pr})_2\text{ATI}]_2\text{SnMe}_2$. Selected bond lengths (Å) and angles (°): Sn–N1, 2.248(4); Sn–N9, 2.267(4); Sn–N16, 2.262(4); Sn–N24, 2.243(4); Sn–C31, 2.163(5); Sn–C32, 2.192(5); N1–Sn–N24, 158.2(1); C32–Sn–C31, 106.3(2); N1–Sn–N9, 71.3(1); N16–Sn–N24, 71.0(1).

$[(\text{Me})_2\text{ATI}]\text{SnMe}_3$ shows coupling between the tin atom and Sn–*Me* protons (^2J = 51.8 Hz), and N–*Me* protons (^3J = 18.4 Hz).

The $[(i\text{-Pr})_2\text{ATI}]\text{SnMe}_3$ has also been synthesized which contains a relatively bulky $[(i\text{-Pr})_2\text{ATI}]^-$ ligand [45]. However, this tin adduct is not stable at room temperature and rearranges cleanly to $[(i\text{-Pr})_2\text{ATI}]_2\text{SnMe}_2$. This transformation can be followed by ^{1}H NMR spectroscopy. Unlike the five coordinate $[(\text{Me})_2\text{ATI}]\text{SnMe}_3$ or $[(i\text{-Pr}_2\text{ATI}]\text{SnMe}_3$ adducts, the six coordinate $[(i\text{-Pr})_2\text{ATI}]_2\text{SnMe}_2$ has a rigid structure in solution as evident from the inequivalent isopropyl groups in the ^{1}H NMR spectrum. Crystalline $[(i\text{-Pr})_2\text{ATI}]_2\text{SnMe}_2$ shows a monomeric structure with an octahedral tin center (Fig. 8).

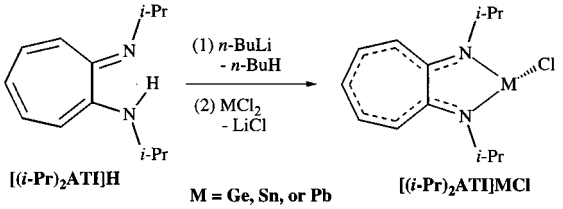

(4)

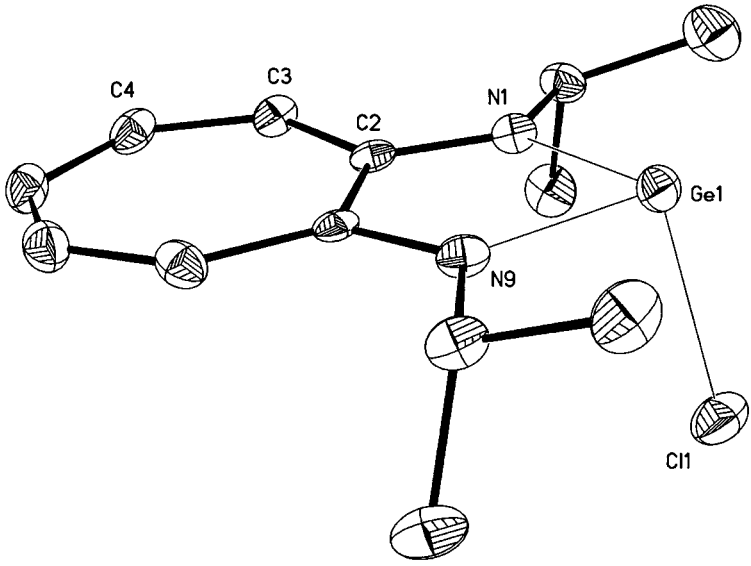

Fig. 9. Molecular structure of {[(*i*-Pr)$_2$ATI]GeCl. Reprinted with permission from Dias et al. [30] © 1997 American Chemical Society. Selected bond lengths (Å) and angles (°): Ge1–N1, 1.956(4); Ge1–N9, 1.956(4); Ge1–Cl1, 2.364(2); N1–C2, 1.338(6); N9–C8, 1.341(6); N1–Ge–N9, 80.2(2); Cl1–Ge–N1, 97.13(13); Cl1–Ge–N9, 96.87(13).

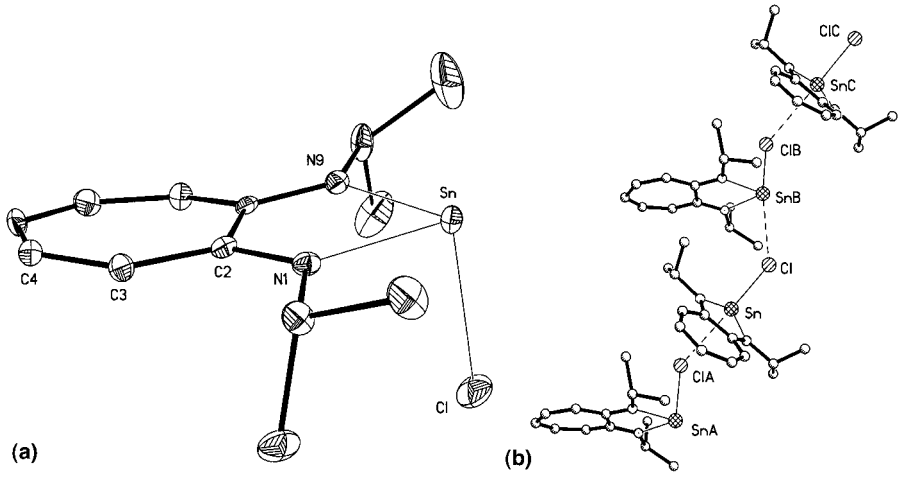

Fig. 10. Molecular structure of {[(*i*-Pr)$_2$ATI]SnCl. **A**. ORTEP diagram. **B**. A view showing intermolecular interactions. Reprinted with permission from Dias et al. [29] © 1996 American Chemical Society. Selected bond lengths (Å) and angles (°): Sn–N1, 2.164(5); Sn–N9, 2.164(5); Sn–Cl, 2.542(2); Sn ⋯ ClA, 3.558; N1–C2, 1.332(7); N9–C8, 1.331(7); N1–Sn–N9, 73.9(2); Cl–Sn–N1, 92.44(13); Cl–Sn–N9, 94.13(12); Cl–Sn ⋯ ClA, 172.3.

Aminotroponiminates are also very useful in low valent group 14 chemistry. A closely related group of compounds of the type [(*i*-Pr_2 ATI]MCl (where M = Ge, Sn and Pb) have been prepared by the reaction between MCl_2 and [(*i*-$Pr)_2$ ATI]Li in 1:1 ratio (Eq. 4) [29,30,42]. They are yellow, crystalline solids. The germanium analog shows a monomeric structure in the solid state (Fig. 9) [30] whereas the tin [29] and lead [45] compounds display chloride bridged zig-zag polymeric chain structures (Figs. 10 and 11, respectively). Metal–Cl and metal–N distances follow the expected order of Pb > Sn > Ge based on the atomic radii. The smallest N1–M–N9 angle in the series was found in the lead analog. The lead adduct shows relatively symmetric metal–Cl separations in the extended structure (e.g. Sn–Cl

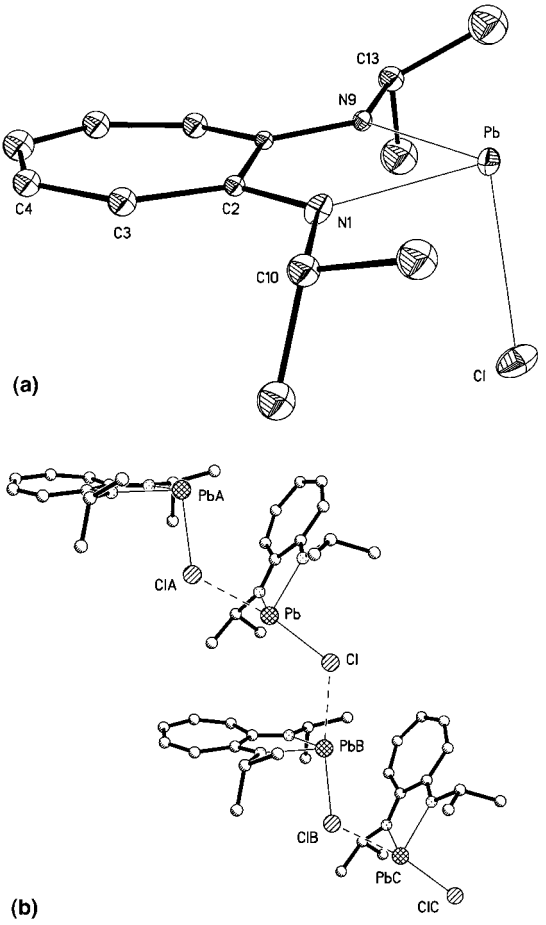

Fig. 11. Molecular structure of {[(*i*-$Pr)_2$ ATI]PbCl. **A**. ORTEP diagram. **B**. A view showing intermolecular interactions. Selected bond lengths (Å) and angles (°): Pb–N1, 2.265(13); Pb–N9, 2.249(13); Pb–Cl, 2.780(4); Pb ··· Cl, 3.095; N1–C2, 1.32(2); N9–C8, 1.33(2); N1–Pb–N9, 70.3(4); Cl–Pb–N1, 91.3(3); Cl–Pb–N9, 95.5(3); Cl–Pb ··· Cl, 170.3.

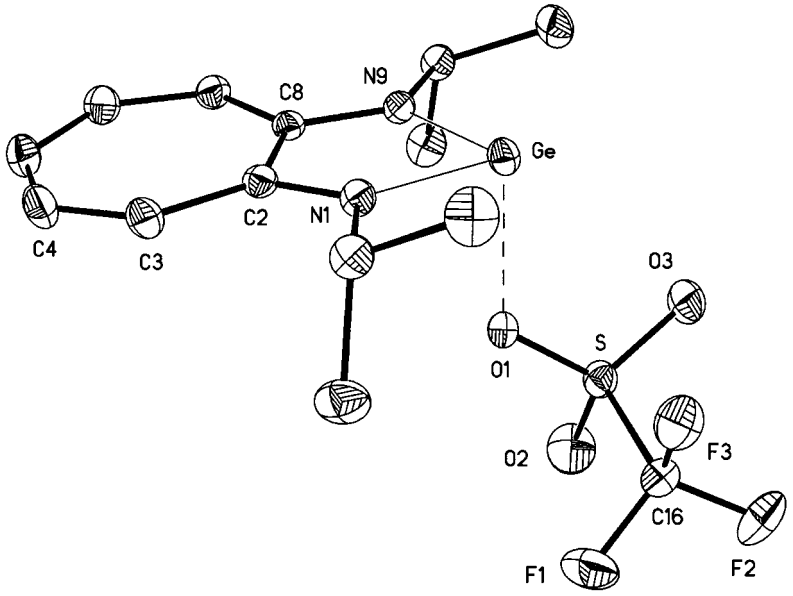

Fig. 12. Molecular structure of {[(*i*-Pr)$_2$ ATI]Ge}[CF_3SO_3]. Reprinted with permission from Dias et al. [30] © 1997 American Chemical Society. Selected bond lengths (Å) and angles (°): Ge–N1, 1.916(2); Ge–N9, 1.910(2); Ge–O, 2.255(2); N1–C2, 1.354(3); N9–C8, 1.352(3); N1–Ge–N9, 81.79(8).

and Sn ⋯ Cl are 2.542 Å and 3.558 Å, respectively, whereas Pb–Cl and Pb ⋯ Cl distances are 2.778 Å and 3.095 Å, respectively). The monochloro germanium species [(Me)$_2$ ATI]GeCl, containing relatively less bulky [(Me)$_2$ ATI]$^-$ ligand, has also been synthesized using $GeCl_2 \cdot$ 1,4-dioxane and the lithium salt of *N,N′*-dimethylaminotroponiminate ligand [30].

The chloride ions of these metal(II) adducts can be replaced by anions such as trifluoromethanesulfonate. For example, the treatment of [(*i*-Pr)$_2$ ATI]GeCl with CF_3SO_3Ag in methylene chloride resulted in the quantitative formation of {[(*i*-Pr)$_2$ ATI]Ge}[CF_3SO_3] (Eq. 5) [30]. The solid state structure shows only a weak Ge ⋯ O interaction (Fig. 12). The Ge–N distances of {[(*i*-Pr$_2$ ATI]Ge}[CF_3SO_3] are

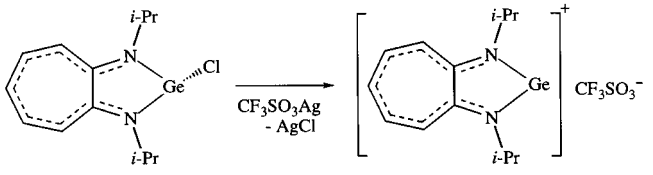

[(*i*-Pr)$_2$ATI]GeCl **{[(*i*-Pr)$_2$ATI]Ge}[CF_3SO_3]** (5)

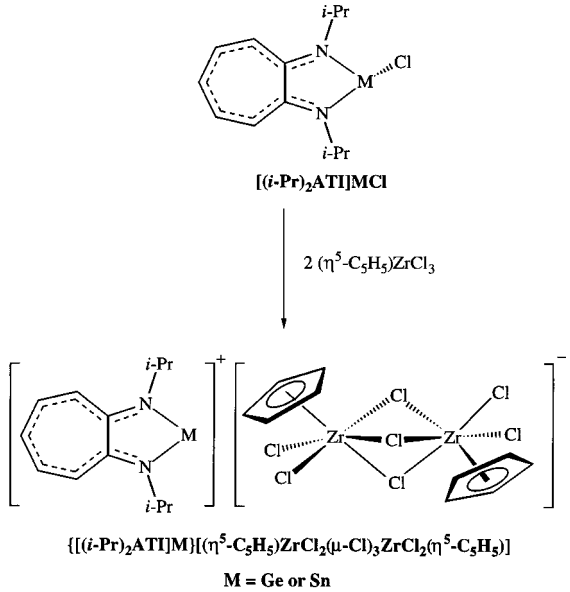

(6)

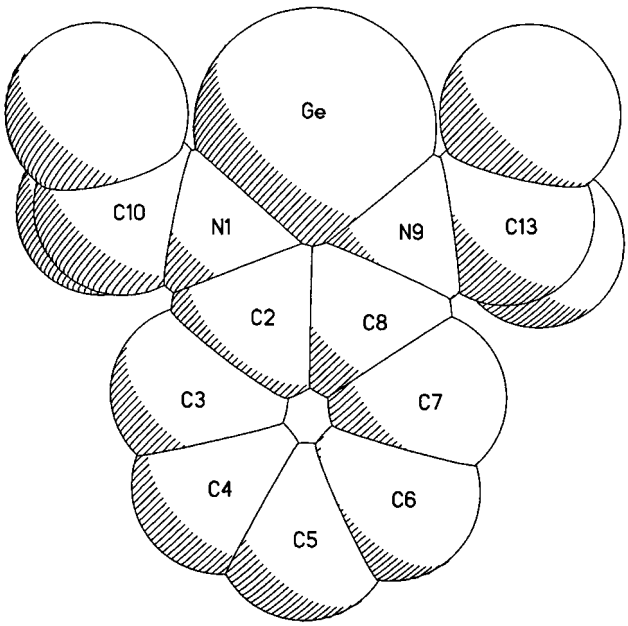

Fig. 13. Molecular structure of $\{[(i\text{-Pr})_2\text{ATI}]\text{Ge}\}^+$ moiety (space filling model). Selected bond lengths (Å) and angles (°): Ge–N1, 1.901(5); Ge–N9, 1.917(5); N1–C2, 1.347(8); N9–C8, 1.346(8); N1–Ge–N9, 81.7(2).

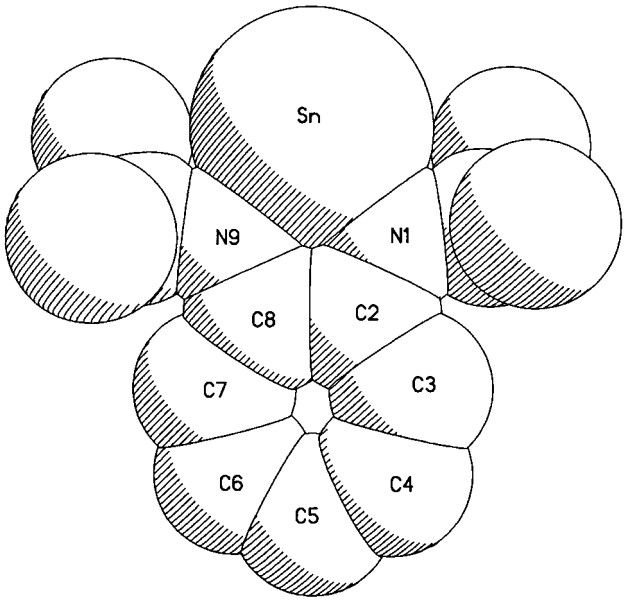

Fig. 14. Molecular structure of $\{[(i\text{-Pr})_2\text{ATI}]\text{Sn}\}^+$ moiety (space filling model). Selected bond lengths (Å) and angles (°): Sn–N1, 2.153(3); Sn–N9, 2.142(3); N1–C2, 1.335(5); N9–C8, 1.341(5); N1–Sn–N9, 74.48(12).

shorter than those found in the $[(i\text{-Pr})_2\text{ATI}]\text{GeCl}$. The ^{1}H NMR data also show notable differences between the chloro and the trifluoromethlysulfonate analog [30].

A very interesting development in group 14 aminotroponiminates concerns the synthesis of two coordinate, cationic Ge and Sn species. The treatment of $[(i\text{-Pr})_2\text{ATI}]\text{GeCl}$ or $[(i\text{-Pr})_2\text{ATI}]\text{SnCl}$ with two equivalents of $(\eta^5\text{-}C_5H_5)ZrCl_3$ in CH_2Cl_2 led to the cationic species $\{[(i\text{-Pr})_2\text{ATI}]\text{Ge}\}[(\eta^5\text{-}C_5H_5)ZrCl_2(\mu\text{-}Cl)_3ZrCl_2(\eta^5\text{-}C_5H_5)]$ or $\{[(i\text{-Pr})_2\text{ATI}]\text{Sn}\}[(\eta^5\text{-}C_5H_5)ZrCl_2(\mu\text{-}Cl)_3ZrCl_2(\eta^5\text{-}C_5H_5)]$ (Eq. 6) [29,30]. The $(\eta^5\text{-}C_5H_5)ZrCl_3$ serves as a chloride abstracting agent in these reactions. These compounds are air and moisture sensitive yellow solids which show moderate solubility in $CHCl_3$ or CH_2Cl_2 but considerably less solubility in hydrocarbon solvents such as hexane or toluene.

$\{[(i\text{-Pr})_2\text{ATI}]\text{Ge}\}[(\eta^5\text{-}C_5H_5)ZrCl_2(\mu\text{-}Cl)_3ZrCl_2(\eta^5\text{-}C_5H_5)]$ and $\{[(i\text{-Pr}_2\text{ATI}]\text{Sn}\}[(\eta^5\text{-}C_5H_5)ZrCl_2(\mu\text{-}Cl_3)ZrCl_2(\eta^5\text{-}C_5H_5)]$ have been characterized by NMR spectroscopy and X-ray crystallography [29,30]. Solid state structures of the cationic moieties are depicted in Figs. 13 and 14. The C_7N_2Ge unit of $\{[(i\text{-Pr})_2\text{ATI}]\text{Ge}\}^+$ is essentially planar. The Ge–N distances are only marginally smaller than those of $[(i\text{-Pr})_2\text{ATI}]\text{GeCl}$. The X-ray structural features of C_7N_2Sn moiety in $[(i\text{-Pr})_2\text{ATI}]\text{SnCl}$ and $\{[(i\text{-Pr})_2\text{ATI}]\text{Sn}\}^+$ are very similar. Solid state data of the cationic germanium and tin species indicate weak interactions between the metal center (Ge or Sn) and chloride ions of the $[(\eta^5\text{-}C_5H_5)ZrCl_2(\mu\text{-}Cl)_3ZrCl_2(\eta^5\text{-}$

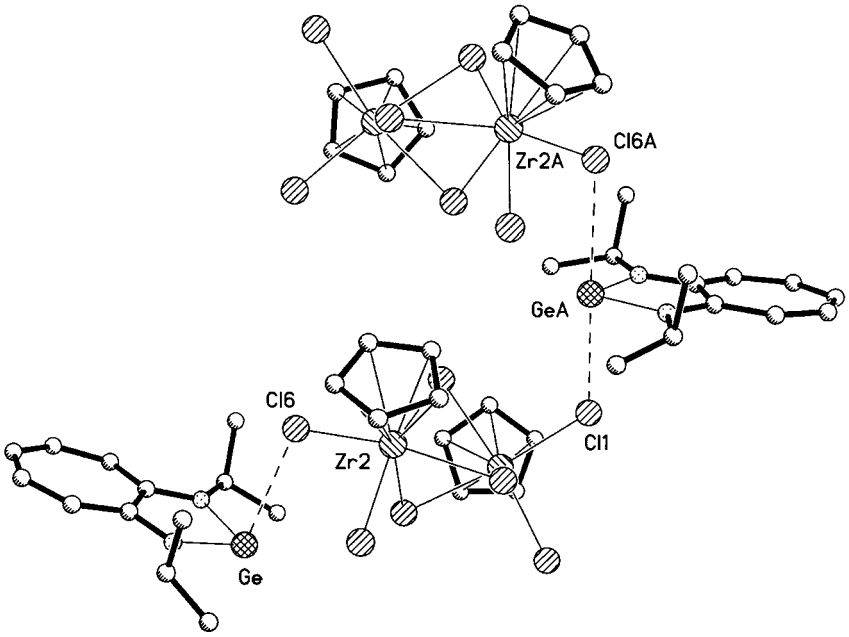

Fig. 15. Molecular structure of {[(*i*-Pr)$_2$ATI]Ge}[(η^5-C_5H_5)$ZrCl_2$(μ-Cl)$_3$$ZrCl_2$($\eta^5$-$C_5H_5$)]. Reprinted with permission from Dias et al. [30] © 1997 American Chemical Society. Ge ··· Cl, 3.115, 3.123; Cl ··· Ge ··· Cl, 169.8.

C_5H_5)]$^-$ anion. These weak interactions lead to zig-zag chain structure in the germanium species (Fig. 15). Tin analog forms centrosymmetric dimers (Fig. 16).

NMR spectroscopic data of these ionic species suggest better ion separation in solution. For example, the ^{119}Sn{^{1}H} NMR resonance of {[(*i*-Pr)$_2$ATI]Sn}[(η^5-C_5H_5)$ZrCl_2$(μ-Cl)$_3$$ZrCl_2$($\eta^5$-$C_5H_5$)] appears at 734 ppm which is significantly different from that of the precursor [(*i*-Pr_2ATI]SnCl (−68 ppm). Furthermore, the ^{119}Sn{^{1}H} NMR chemical shift of {[(*i*-Pr)$_2$ATI]Sn}[(η^5-C_5H_5)$ZrCl_2$(μ-Cl)$_3$$ZrCl_2$($\eta^5$-$C_5H_5$)] is very close to the values observed for two-coordinate tin amides such as [$(Me_3Si)_2N]_2Sn$ (759 ppm) [46], $(Me_3Si)_2NSnN(SiMe_3)C_6H_{10}(SiMe_3)NSnN(SiMe_3)_2$ (694 ppm) [47] or $Me_2Si[N(Bu^t)]_2Sn$ (638 ppm) [46].

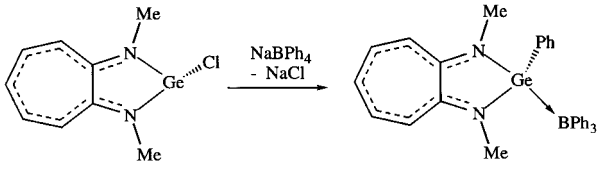

[(Me)$_2$ATI]GeCl **[(Me)$_2$ATI]GePh•BPh$_3$** (7)

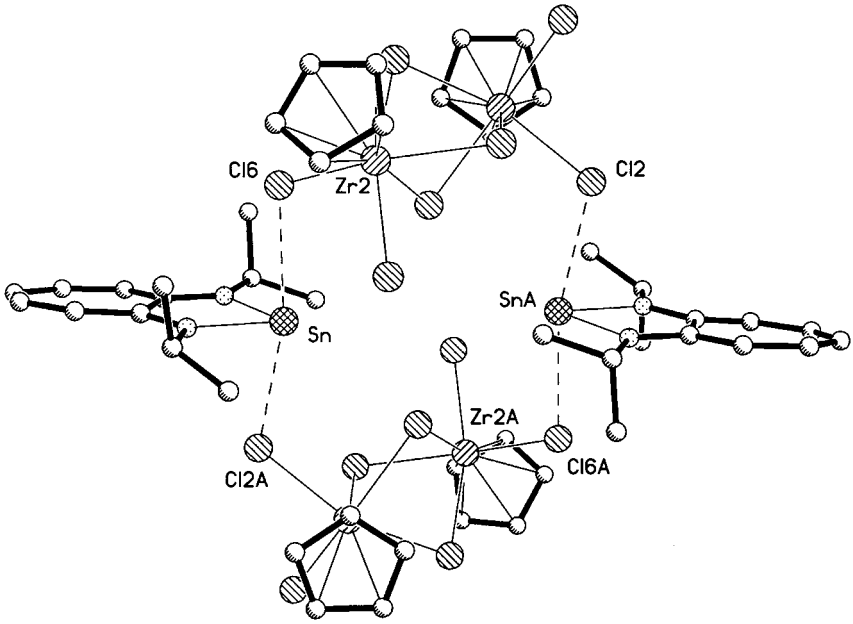

Fig. 16. Molecular structure of {[(*i*-Pr)$_2$ ATI]Sn}[(η^5-C_5H_5)$ZrCl_2$(μ-Cl)$_3$$ZrCl_2$($\eta^5$-$C_5H_5$)]. Reprinted with permission from Dias et al. [29] © 1996 American Chemical Society. Sn ⋯ Cl, 2.979, 3.123; Cl ⋯ Sn ⋯ Cl, 166.1.

The reaction between [(Me)$_2$ ATI]GeCl and $NaBPh_4$ did not result in the expected tetraphenylborate salt of {[(Me)$_2$ ATI]Ge}$^+$. Instead, it resulted in the formation of a phenyl group transfer product [(Me)$_2$ ATI]GePh · BPh_3 (Eq. 7) [30].

Bis-ligand complex [(Me)$_2$ ATI]$_2$Sn has been synthesized by treating [(Me)$_2$ ATI]H with bis[bis(trimethylsilyl)amido]tin(II) (Eq. 8), and characterized by NMR spectroscopy and X-ray crystallography [12]. It shows a distorted pseudo-trigonal bipyramidal geometry at the tin center (Fig. 17). The stereochemically active lone pair on tin(II) presumably occupies an equatorial site. Long intermolecular Sn ⋯ Sn contacts (3.769 Å) have also been observed in the solid state (Fig. 18). This tin adduct shows fluxional behavior in solution at ambient temperatures.

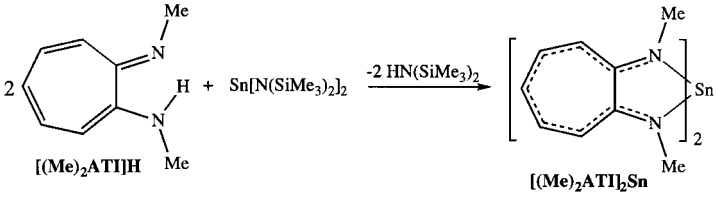

(8)

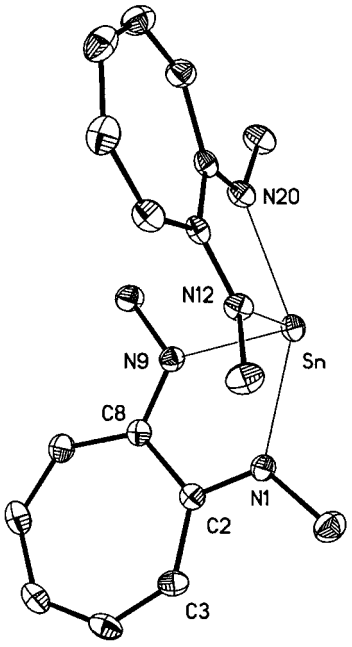

Fig. 17. Molecular structure of $[(Me)_2ATI]_2Sn$. Reprinted with permission from Dias and Jin [12] © 1996 American Chemical Society. Selected bond lengths (Å) and angles (°): Sn–N1, 2.301(2); Sn–N9, 2.225(2); Sn–N12, 2.215(2); Sn–N20, 2.295(2); N1–Sn–N20, 144.85(8); N9–Sn–N12, 94.41(8); N1–Sn–N9, 69.29(8); N20–Sn–N12, 69.72(8).

Very little is known about the reactivity of these group 14 complexes. A ligand transfer ability of $[(Me)_2ATI]_2Sn$ has been reported [12]. It undergoes oxidative ligand transfer reactions with GaI and InCl leading to $[(Me)_2ATI]_2GaI$ and $[(Me)_2ATI]_2InCl$, respectively.

4. Conclusion

The availability of a variety of *N*,*N*′-disubstututed analogs combined with the relatively robust ligand backbone and the powerful chelating ability makes aminitroponimines ideal ligands for many applications. However, very little is known about their main group coordination chemistry [11,12,29,30,40,42,45,48,49]. Among the main group adducts of aminotroponiminates, group 14 derivatives have attracted the most interest (with group 13 derivatives close behind). The neutral aminotroponimines and their alkali metal adducts serve as excellent precursors for the synthesis of both high and low valent group 14 derivatives. Resulting adducts feature mostly planar, heterobicyclic 10π-electron C_7N_2M ring systems. Aminotroponiminates also allow the isolation of low valent, low coordinate Ge and

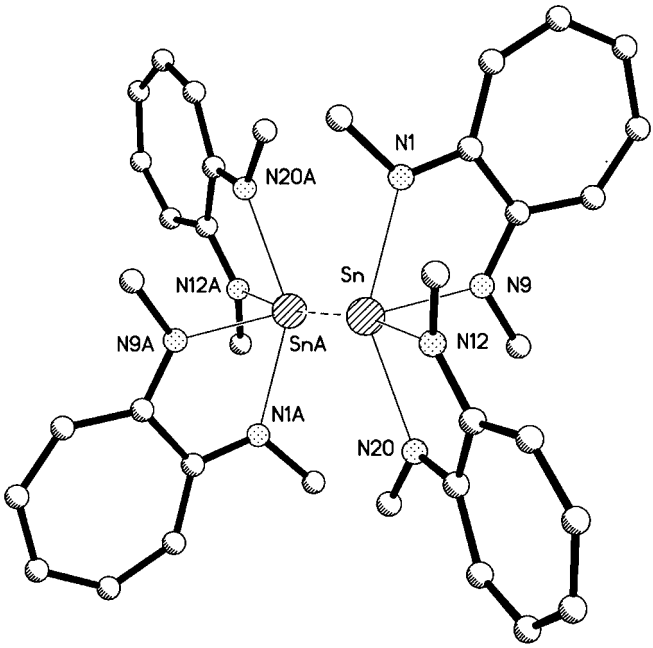

Fig. 18. A view of $[(Me)_2ATI]_2Sn$ showing Sn ··· Sn intermolecular interaction.

Sn species. Structures, bonding and chemistry of such species are of significant interest. Some of the aminotroponiminato group 14 derivatives are also promising ligand transfer agents. Based on the current level of development as evident from this review, it is quite apparent that the group 14 aminotroponiminato chemistry is still in its infancy.

Acknowledgements

We thank the Donors of The Petroleum Research Fund, administered by the American Chemical Society, The Robert A. Welch Foundation, and The University of Texas at Arlington for support of work carried out at UTA.

References

[1] R.E. Brasen, J. Am. Chem. Soc. 82 (1960) 5948.
[2] W.R. Brasen, H.E. Holmquist, R.E. Benson, J. Am. Chem. Soc. 83 (1961) 3125.
[3] W.R. Brasen, H.E. Holmquist, R.E. Benson, J. Am. Chem. Soc. 82 (1960) 995.
[4] R.H. Holm, M.J. O'Connor, Prog. Inorg. Chem. 14 (1971) 241, and references therein.
[5] S. Imajo, K. Nakanishi, M. Roberts, S.J. Lippard, T. Nozoe, J. Am. Chem. Soc. 105 (1983) 2071.
[6] M. Schumann, H. Elias, Inorg. Chem. 24 (1985) 3187.

[7] H. Brunner, A. Knott, R. Benn, A. Rufinska, J. Organomet. Chem. 295 (1985) 211.
[8] A. Zask, N. Gonnella, K. Nakanishi, C.J. Turner, S. Imajo, T. Nozoe, Inorg. Chem. 25 (1986) 3400.
[9] K. Shindo, H. Wakabayashi, H. Miyamae, S. Ishikawa, T. Nozoe, Heterocycles 37 (1994) 943.
[10] G.M. Villacorta, S.J. Lippard, Pure Appl. Chem. 58 (1986) 1477.
[11] H.V.R. Dias, W. Jin, R.E. Ratcliff, Inorg. Chem. 34 (1995) 6100.
[12] H.V.R. Dias, W. Jin, Inorg. Chem. 35 (1996) 6546.
[13] F.T. Edelmann, Coord. Chem. Rev. 137 (1994) 403.
[14] P.B. Hitchcock, M.F. Lappert, D.-S. Liu, J. Chem. Soc., Chem. Commun. (1994) 1699; W. Clegg, S.J. Coles, E.K. Cope, F.S. Mair, Angew. Chem., Int. Ed. Engl. 37 (1998) 796, and references therein.
[15] Cambridge Structural Database, Cambridge, January, 1996, and references therein.
[16] G.M. Villacorta, C.P. Rao, S.J. Lippard, J. Am. Chem. Soc. 110 (1988) 3175.
[17] B.S. Jaynes, T. Ren, S. Liu, S.J. Lippard, J. Am. Chem. Soc. 114 (1992) 9670.
[18] B.S. Jaynes, T. Ren, A. Masschelein, S.J. Lippard, J. Am. Chem. Soc. 115 (1993) 5589.
[19] G.M. Villacorta, S.J. Lippard, Inorg. Chem. 27 (1988) 144.
[20] G.M. Villacorta, D. Gibson, I.D. Williams, S.J. Lippard, J. Am. Chem. Soc. 107 (1985) 6732.
[21] W.M. Davis, A. Zask, K. Nakanishi, S.J. Lippard, Inorg. Chem. 24 (1985) 3737.
[22] W.M. Davis, M.M. Roberts, A. Zask, K. Nakanishi, T. Nozoe, S.J. Lippard, J. Am. Chem. Soc. 107 (1985) 3864.
[23] M. Bartlett, G.J. Palenic, J. Chem. Soc. D. (1970) 416.
[24] D.R. Eaton, A.D. Josey, R.E. Benson, J. Am. Chem. Soc. 89 (1967) 4040.
[25] D.R. Eaton, W.R. McClellan, J.F. Weiher, Inorg. Chem. 7 (1968) 2040.
[26] H.V.R. Dias, W. Jin, Z. Wang, Inorg. Chem. 35 (1996) 6074.
[27] M.J. Scott, S.J. Lippard, J. Am. Chem. Soc. 119 (1997) 3411.
[28] M.J. Scott, S.J. Lippard, Inorg. Chim. Acta 263 (1997) 287.
[29] H.V.R. Dias, W. Jin, J. Am. Chem. Soc. 118 (1996) 9123.
[30] H.V.R. Dias, Z. Wang, J. Am. Chem. Soc. 119 (1997) 4650.
[31] T. Nozoe, M. Sata, K. Ito, K. Matsui, T. Matsuda, Proc. Jpn. Acad. 29 (1953) 565.
[32] I. Murata, Bull. Chem. Soc. Jpn. 32 (1959) 841.
[33] J.J. Drysdale, W.W. Gilbert, H.K. Sinclair, W.H. Sharkey, J. Am. Chem. Soc. 80 (1958) 3672.
[34] H. Nakao, Chem. Pharm. Bull. (Tokyo) 13 (1965) 810.
[35] N. Soma, J. Nakazawa, T. Watanabe, Y. Sato, G. Sunagawa, Chem. Pharm. Bull. (Tokyo) 13 (1965) 819.
[36] C.E. Forbes, R.H. Holm, J. Am. Chem. Soc. 90 (1968) 6884.
[37] K.-H. Ahn, R.B. Klassen, S.J. Lippard, Organometallics 9 (1990) 3178.
[38] P. Goldstein, K.N. Trueblood, Acta Crystallogr. 23 (1967) 148.
[39] S.G. Bott, K.-H. Ahn, S.J. Lippard, Acta Crystallogr. C45 (1989) 1738.
[40] E.L. Muetterties, C.M. Wright, J. Am. Chem. Soc. 86 (1964) 5132.
[41] D.R. Eaton, W.R. McClellan, Inorg. Chem. 6 (1967) 2134.
[42] H.V.R. Dias, Z. Wang, unpublished results.
[43] P.W. Roesky, Chem. Ber./Recueil 130 (1997) 859.
[44] E.L. Muetterties, US Patent 3,177,232 (1965).
[45] H.V.R. Dias, W. Jin, unpublished results.
[46] B. Wrackmeyer, J. Schiller, Z. Naturforsch. 47 (1992) 662.
[47] H. Braunschweig, P.B. Hitchcock, M.F. Lappert, L.J.-M. Pierssens, Angew. Chem., Int. Ed. Engl. 33 (1994) 1156.
[48] H.E. Holmquist, R.E. Benson, J. Am. Chem. Soc. 84 (1962) 4720.
[49] H.V.R. Dias, W. Jin, J. Chem. Crystallogr. 27 (1997) 353.